Computational Sonography

Christoph Hennersperger[1], Maximilian Baust[1],
Diana Mateus[1], and Nassir Navab[1,2]

[1] Computer Aided Medical Procedures, Technische Universität München, Germany
[2] Computer Aided Medical Procedures, Johns Hopkins University, USA
christoph.hennersperger@tum.de

Abstract. 3D ultrasound imaging has high potential for various clinical applications, but often suffers from high operator-dependency and the directionality of the acquired data. State-of-the-art systems mostly perform compounding of the image data prior to further processing and visualization, resulting in 3D volumes of scalar intensities. This work presents computational sonography as a novel concept to represent 3D ultrasound as tensor instead of scalar fields, mapping a full and arbitrary 3D acquisition to the reconstructed data. The proposed representation compactly preserves significantly more information about the anatomy-specific and direction-depend acquisition, facilitating both targeted data processing and improved visualization. We show the potential of this paradigm on ultrasound phantom data as well as on clinically acquired data for acquisitions of the femoral, brachial and antebrachial bone.

1 Introduction

Tracked freehand 3D ultrasound (US) yields 3D information of the scanned anatomy by acquiring 1D scanlines or 2D images, respectively, along with their position and orientation in space. For further processing and visualization, the data is then often interpolated with respect to a regular grid. This procedure is commonly referred to as 3D reconstruction or *compounding* [10] and can be performed in different ways, *e.g.* forward, backward or functional interpolation. All these approaches reconstruct scalar intensity values per voxel,however, such conventional compounding techniques suffer from two inconveniences.

First, they imply a significant loss of information and neglect the directionality-dependent nature of ultrasound. Second, in order to avoid artifacts, they impose acquisition protocols (*e.g.* straight probe motion) modifying the physician's common practice (acquisition guided by interactive motion of the probe).

In this work we propose a novel paradigm for 3D US representation, called *Computational Sonography* (CS), based on the the reconstruction of tensor fields instead of the traditional intensity volumes, *cf.* Fig. 1. In our approach, at every 3D location a 2nd order tensor is optimized to compactly encode the amount of reflected signal expected from each direction. In this way, both the anatomy- and the acquisition-specific directionalities are preserved.

N. Navab et al. (Eds.): MICCAI 2015, Part II, LNCS 9350, pp. 459–466, 2015.
DOI: 10.1007/978-3-319-24571-3_55

The advantages of this novel reconstruction paradigm are as follows:

1. It preserves directional information while allowing for the retrieval of scalar intensity volumes for arbitrary directions. This calls for novel (interactive) visualization techniques which better reflect the directional nature of US.
2. The proposed reconstruction paradigm can be applied to arbitrary scanning trajectories. Thus, the clinician is not subjected to strict scanning protocols.
3. The presented method is fast in terms of reconstruction time (easily parallelizable), while leading to a compact representation (constant storage/voxel).
4. Beyond visualization, the preserved information in CS provides additional value for tasks where 3D ultrasound is used for further processing, *e.g.* registration, segmentation or tracking [6,3,13]. Furthermore, CS also enables using post-processing techniques specialized to tensor-valued data, *e.g.* [12].

The proposed method is inspired by *computational photography*, where light fields instead of just intensities are stored and available to subsequent processing steps [8]. Our vision is that tensor fields become the standard format for freehand 3D US acquisitions, enabling a plenitude of novel computational techniques. We demonstrate the potential of this new paradigm for both phantom and in-vivo data and compare it to state-of-the-art compounding methods.

Related Work: A popular and successful example of tensor fields is Diffusion Tensor Imaging (DTI), for which a vast literature addressing tensor fitting,

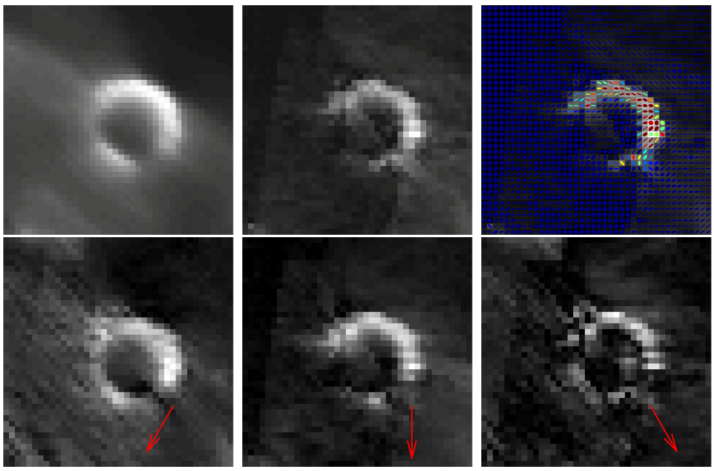

Fig. 1. Top: Reconstruction Comparison. (left) Conventional reconstruction from arbitrarily sampled vascular ultrasound data obtained by backward-interpolation using median compounding. **(middle)** Absolute value of the trace of the reconstructed tensors. **(right)** Tensors visualized as colored ellipses. Note that the trace image nicely resembles the high intensities of the boundary and that tensors align with the global orientation of the imaged structures. **Bottom: Directionality of Tensors.** Reconstructed tensors allow for a reconstruction of directional B-Mode ultrasound information in arbitrary directions, as indicated by red arrows.

visualization, *etc.* [7] exists. In contrast to DTI, compounding of freehand 3D US data is today only considered in terms of reconstructing scalar intensity volumes [10], which neglects most of the directional information acquired along the trajectory of the scan. Recently, a method for incorporating directionality of ultrasound acquisitions was proposed, clustering data from different directions for 3D compounding [1]. While this method utilizes information from different directions for a combined reconstruction, it still reconstructs only scalar values per voxel, and thus directional information is not available for further processing. In [9], the spatial coherence of ultrasound information observed for different orientations and focal regions has been used for tensor reconstructions. While the method is promising, it requires both a specialized hardware setup and a fixed scanning protocol. In contrast, our approach can be seamlessly integrated into the clinical workflow and applied directly to clinical 3D ultrasound acquisitions. Furthermore, the reconstructed tensor fields result in a compact representation of the directional information observed during the acquisition, which remains available for subsequent processing tasks.

2 Computational Sonography for 3D Ultrasound

The basis for any 3D ultrasound reconstruction is a set of ultrasound samples $S = \{s_i\}_i^N$. The samples typically lie on rays (scanlines) that are more or less arbitrarily distributed in 3D space based on the acquisition trajectory. Each sample, denoted here by s_i, is given by a tuple $s_i = \{I_i, p_i, v_i\}$ consisting of the ultrasound intensity I_i, the sample position $p_i = (p_{i,x}, p_{i,y}, p_{i,z})^\top$ and the corresponding ray direction $v_i = (v_{i,x}, v_{i,y}, v_{i,z})^\top$. Current 3D ultrasound techniques use only intensities I_i and positions p_i to reconstruct 3D intensity volumes. Because the content of ultrasound images is direction-dependent, we argue that preserving the directionality is both important and beneficial, which calls for a paradigm change in US data representation. We propose here to rely on tensors to encode such complex behavior, as this resembles the anisotropic nature of ultrasound waves best, with varying visibility of structures and a change penetration depth using different scanning trajectories. The key idea of Computational Sonography is thereby to reconstruct a 3D tensor field from the collection of samples S, where each tensor will compactly and optimally encode the local intensity for each viewing direction. In practice, to reconstruct tensor data from the samples, a two-step approach is proposed, comprising of a selection of US samples in proximity to the respective voxel, followed by the tensor reconstruction through least-squares minimization, *cf.* Fig. 2.

2.1 Sample Selection

At first, we select the subset of the ultrasound samples $s_i \in S$ which contribute to the tensor estimation at a specific volume point $p = (p_x, p_y, p_z)^\top \in P$. Here $P \in \mathbb{Z}^3$ denotes the lattice (set of positions) at which the tensors shall be reconstructed. A proper selection of the respective subset of samples is important,

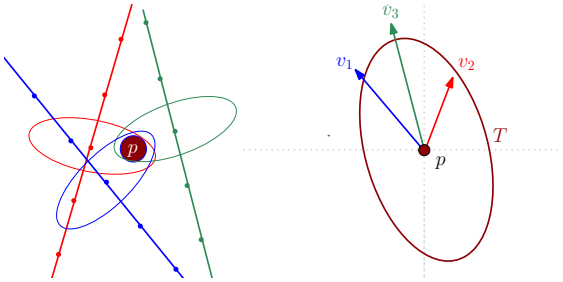

Fig. 2. Reconstruction Process: (left) Ultrasound sample selection from a set of samples close to the target volume position. **(right)** Reconstruction of a 2nd order tensor from measurements originating from different ultrasound rays.

because (i) the selected samples should contain complementary information, i.e., the corresponding measurements should be independent, and ii) potential outliers should be removed in order to avoid a distortion of the subsequent tensor estimation. In this regard and inspired by [2], all input samples S are traversed and a sample s_i is selected if p_i lies within an ellipsoid defined around the ultrasound sample, *cf.* left panel in Fig. 2:

$$\left(\frac{p_x - p_{i,x}}{a}\right)^2 + \left(\frac{p_y - p_{i,y}}{b}\right)^2 + \left(\frac{p_z - p_{i,z}}{c}\right)^2 \leq 1, \tag{1}$$

where a, b, c represent the maximum distances in the native sampling space in x-, y-, and z-direction, respectively. This sample selection w.r.t. the coordinate systems of the original ultrasound rays (in a backward fashion) is of special interest if physical parameters of an acquisition, such as frequency, probe element width, height, pitch, or focus, are incorporated into the reconstruction approach. Based on Eq. (1), multiple samples of each scan line would be selected depending on the proximity of a ray to the target position p. As better tensor reconstructions can be obtained from complementary information, only the nearest sample of each ray is selected instead of all samples fulfilling (1), thus restricting the set to contain only one sample per scanline.

2.2 Tensor Reconstruction

As a result of the sample selection, every voxel position p has an assigned set of samples $s_1, \ldots, s_n \subset S$, which can be used for the reconstruction of a tensor $T \in \mathbb{R}^{3\times3}$. In our CS conception, the 3D reconstruction should be able to reproduce as faithfully as possible the directionality dependence of the acquisition. To this end, we assume that for each sample s_i, ideally the following relationship holds:

$$v_i^\top T v_i = I_i, \quad \text{where} \quad T = \begin{bmatrix} T_{xx} & T_{xy} & T_{xz} \\ T_{xy} & T_{yy} & T_{yz} \\ T_{xz} & T_{yz} & T_{zz} \end{bmatrix}. \tag{2}$$

This results in the recovery of the tensor that preserves the intensities for each orientation best, given the sample subset assigned to the voxel. If estimated properly, it will then be possible to retrieve an intensity volume for an arbitrary viewing direction $v \in \mathbb{R}^3$ by evaluating the tensor w.r.t. this direction, i.e., by computing $v^\top T v$ at all voxel positions.

As T shall be symmetric, it is possible to rewrite (2) as follows:

$$\left[\, v_{i,x}^2,\, v_{i,y}^2,\, v_{i,z}^2,\, 2v_{i,x}v_{i,y},\, 2v_{i,x}v_{i,z},\, 2v_{i,y}v_{i,z} \,\right] \left[\, T_{xx}\; T_{yy}\; T_{zz}\; T_{xy}\; T_{xz}\; T_{yz} \,\right]^\top = I_i. \tag{3}$$

This means that we need at least six sampling points in order to compute the six coefficients T_{xx}, T_{yy}, T_{zz}, T_{xy}, T_{xz}, and T_{yz}. In practice, however, we use more than six samples, typically between 12 and 500 samples. As a consequence, we end up with a least squares problem

$$\|Ax - b\|_2^2\,, \tag{4}$$

where the i-th entry of $b \in \mathbb{R}^n$ is given by I_i, the i-th row of $A \in \mathbb{R}^{n\times 6}$ is given by $(v_{i,x}^2, v_{i,y}^2, v_{i,z}^2, 2v_{i,x}v_{i,y}, 2v_{i,x}v_{i,z}, 2v_{i,y}v_{i,z})^\top$, and $x \in \mathbb{R}^6$ denotes the solution vector. We solve this least squares problem for all volume points simultaneously using Cholesky decompositions implemented on a GPU.

At this point it is important to note that the symmetry of T is ensured by the used parametrization (3). However, as intensities are expected to be positive, T should be positive definite ($v^\top T v > 0$), which is not yet enforced in our scheme. This can partially result in erroneous tensor estimates, especially in areas with severe shadows or almost no meaningful information. We suggest to detect these areas by means of other approaches, *e.g.* by computing confidence values as suggested by [4], and exclude them from further processing.

3 Experimental Evaluation

For evaluating the potential of computational sonography as a new paradigm for 3D ultrasound reconstruction, we performed experiments on both phantom and in-vivo data. All 3D freehand image acquisitions were performed with an Ultrasonix RP system and a linear transducer (L14-5/38) tracked with an Ascension EM system. For the relevant sample selection, we chose $a = b = c = 1.5\ mm$. Volumetric spacing can be chosen freely as a balance between reconstruction quality (finer spacing) and speed (coarser); here all datasets were reconstructed with a spacing of 0.5mm in accordance with previous work. One advantage of computational sonography is the possibility to directly reconstruct information w.r.t. any viewing direction v by evaluating all the tensors according to $v^\top T v$, yielding an intensity volume corresponding to the direction v. Storing an acquired US sweep as a tensor volume thus facilitates the optimal resembling of the directional nature of ultrasound in any kind of interactive visualization for instance. As this possibility is conceptually similar to computational photography and particularly light field imaging, where the focus plane can be chosen

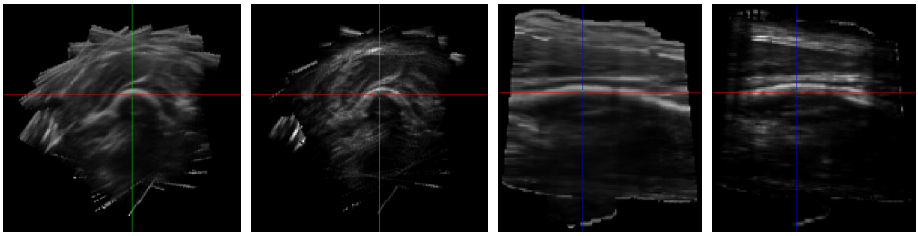

Fig. 3. Comparison of 3D Reconstructions - Real Data: Transverse **(column 1)** and longitudinal **(column 3)** slices for median compounding and similarly for the absolute value of the tensor trace of our reconstruction **(columns 2,4)** from a rotational scan of the Brachial bone. Note that conventional compounding depicts mainly the bone structure, while our reconstruction better resembles the overall structures in the volume.

and modified after the image acquisition process, we chose the term *computational sonography*. It can be observed in Fig. 3 and Fig. 4 that this procedure yields high quality reconstructions. Considering the directional information thus results in the possibility to retrieve texture information as it would be observed from arbitrarily chosen directions, in comparison to conventional reconstruction approaches which do not take directional information into account. In particular for Fig. 3, the median-reconstructed frame does not show anatomical information except for the shadowing/bone. Moreover, it is also distorted due to components from different views. In contrast to this, *computational sonography* allows for a reconstruction of directional information, preserving the original image information. It should be noted that the lack of speckle patterns in both images is mainly due to the large cell size (0.5mm with ∼500samples/voxel).

In order to demonstrate this effect also quantitatively, we reconstructed volumes for different acquisitions using the orientations of the corresponding original images. For evaluation, we compared the reconstructed intensity values with the original ultrasound samples, where we used the Mean Absolute Distance (MAD) to the original US image as well as the Peak Signal to Noise Ratio (PSNR) as evaluation metrics. As a baseline method, we employed the median compounding strategy, which is often recommended due to its preservation of the original US image appearance [11]. We performed this evaluation on two different sets of data: i) Five freehand scans of an in vitro silicone vessel phantom immersed in gelatin (2% gelatin, 1% agar, 1% flour) in order to allow for a scanning of realistic anatomies in a static environment, and ii) Ten freehand scans of the Femoral bone as well as the Antebrachial and Brachial bones using varying trajectories to evaluate the feasibility in a realistic setup. For both sets, we performed acquisitions using rotationally and overlapping trajectories, where a target volume position is imaged several times from different directions as this scenario well resembles the daily routine for US diagnostics. We perform a quantitative evaluation on 5 datasets (avg. 167 ± 103 slices) for the silicone phantom and 10 in-vivo datasets (avg. 243 ± 84 slices). Table 1 shows that CS provides on average higher peak SNR values as well as slightly lower absolute

Table 1. Quantitative results

	Phantom		In-vivo	
Method	MAD	PSNR	MAD	PSNR
Median Compounding	17.70 ± 1.81	20.31 ± 0.91	20.79 ± 2.27	18.67 ± 0.97
Computational Sonography	17.46 ± 2.47	57.67 ± 8.79	19.64 ± 2.89	66.35 ± 9.43

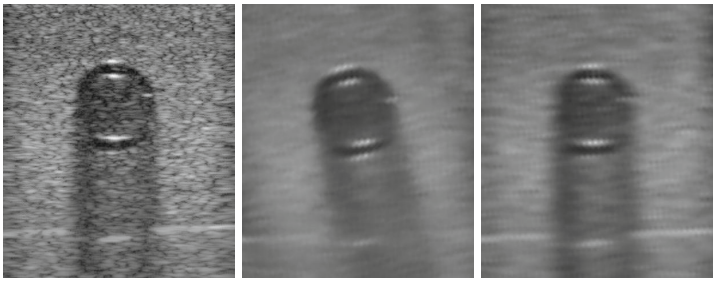

Fig. 4. Consistency with Original Acquisitions - Phantom Data: (left) Original B-mode image from a scan of the vessel phantom. **(middle)** Conventional reconstruction using median compounding. **(right)** Result computed from the proposed tensor representation using the direction v corresponding to the original image. Note the significant loss of original information in case of the regular compounding.

distances, while being partially susceptible to varying imaging conditions, as indicated by increased PSNR variability for CS. Observed high PSNR values show the potential of computational sonography as a new paradigm in 3D ultrasound imaging. Our future work includes enforcing the positive definiteness of T [5] to improve the results and developing a more efficient implementation (for a spacing of 0.5mm, the computational time is about 4 minutes per volume).

4 Conclusion

In this work we presented *computational sonography* as new paradigm for 3D ultrasound, reconstructing tensor fields from the acquired data instead of scalar intensities being used in today's practice. For tensor retrieval, we propose a two-step approach with a sample selection performed first, followed by a tensor reconstruction through least-squares solution. Our results show that the approach preserves the original (B-mode) ultrasound data better compared to state-of-art methods and yields a high potential for utilization of tensor information in further processing and visualization steps. With improved reconstruction schemes such as tensor fitting with direct regularization, as used frequently in DTI, computational sonography will hopefully evolve as a standard for reconstruction of 3D ultrasound data in the future. Applications that could benefit from our new representation are: multi-modal registration, segmentation, tracking, free viewpoint approximation (e.g. for educational simulation), online guidance of the

acquisition to optimize the 3D reconstruction as well as analysis and comparison of different acquisitions. The additional information can be further used online to guide the current acquisition, e.g. acoustic window optimization, or offline, enabling targeted image analysis by allowing different users to extract different relevant information based on their technical or clinical objectives.

References

1. zu Berge, C.S., Kapoor, A., Navab, N.: Orientation-driven ultrasound compounding using uncertainty information. In: Stoyanov, D., Collins, D.L., Sakuma, I., Abolmaesumi, P., Jannin, P. (eds.) IPCAI 2014. LNCS, vol. 8498, pp. 236–245. Springer, Heidelberg (2014)
2. Hennersperger, C., Karamalis, A., Navab, N.: Vascular 3D+T freehand ultrasound using correlation of doppler and pulse-oximetry data. In: Stoyanov, D., Collins, D.L., Sakuma, I., Abolmaesumi, P., Jannin, P. (eds.) IPCAI 2014. LNCS, vol. 8498, pp. 68–77. Springer, Heidelberg (2014)
3. Hu, N., Downey, D.B., Fenster, A., Ladak, H.M.: Prostate boundary segmentation from 3D ultrasound images. Medical Physics 30(7), 1648–1659 (2003)
4. Karamalis, A., Wein, W., Klein, T., Navab, N.: Ultrasound confidence maps using random walks. Medical Image Analysis 16(6), 1101–1112 (2012)
5. Koay, C.G., Chang, L.-C., Carew, J.D., Pierpaoli, C., Basser, P.J.: A unifying theoretical and algorithmic framework for least squares methods of estimation in diffusion tensor imaging. Journal of Magnetic Resonance 182(1), 115 (2006)
6. Lang, A., Mousavi, P., Gill, S., Fichtinger, G., Abolmaesumi, P.: Multi-modal registration of speckle-tracked freehand 3D ultrasound to ct in the lumbar spine. Medical Image Analysis 16(3), 675–686 (2011)
7. Le Bihan, D., Mangin, J.F., Poupon, C., Clark, C.A., Pappata, S., Molko, N., Chabriat, H.: Diffusion tensor imaging: concepts and applications. Journal of Magnetic Resonance Imaging 13(4), 534–546 (2001)
8. Ng, R., Levoy, M., Brédif, M., Duval, G., Horowitz, M., Hanrahan, P.: Light field photography with a hand-held plenoptic camera. Computer Science Technical Report CSTR 2(11) (2005)
9. Papadacci, C., Tanter, M., Pernot, M., Fink, M.: Ultrasound backscatter tensor imaging (BTI): analysis of the spatial coherence of ultrasonic speckle in anisotropic soft tissues. IEEE Transactions on Ultrasonics, Ferroelectrics and Frequency Control 61(6), 986–996 (2014)
10. Solberg, O.V., Lindseth, F., Torp, H., Blake, R.E., Nagelhus Hernes, T.A.: Freehand 3D ultrasound reconstruction algorithms - a review. Ultrasound in Medicine and Biology 33, 991–1009 (2007)
11. Wein, W., Pache, F., Röper, B., Navab, N.: Backward-warping ultrasound reconstruction for improving diagnostic value and registration. In: Larsen, R., Nielsen, M., Sporring, J. (eds.) MICCAI 2006. LNCS, vol. 4191, pp. 750–757. Springer, Heidelberg (2006)
12. Weinmann, A., Demaret, L., Storath, M.: Total Variation Regularization for Manifold-Valued Data. SIAM Journal on Imaging Sciences 7(4), 2226–2257 (2014)
13. Yang, L., Georgescu, B., Zheng, Y., Meer, P., Comaniciu, D.: 3D ultrasound tracking of the left ventricle using one-step forward prediction and data fusion of collaborative trackers. In: IEEE Conf. on Comp. Vision and Pattern Recognition (2008)